World Electric Vehicle Journal

MDPI

Article

Integrating Vehicle-to-Infrastructure Communication for Safer Lane Changes in Smart Work Zones

Mariam Nour [1,*], Mayar Nour [2] and Mohamed H. Zaki [2]

[1] Civil, Environmental and Construction Engineering Department, University of Central Florida, Orlando, FL 32835, USA
[2] Department of Civil and Environmental Engineering, Western University, London, ON N6A 3K7, Canada; mnour6@uwo.ca (M.N.); m.zaki@uwo.ca (M.H.Z.)
* Correspondence: mariam.nour@ucf.edu

Abstract: As transportation systems evolve, ensuring safe and efficient mobility in Intelligent Transportation Systems remains a priority. Work zones, in particular, pose significant safety challenges due to lane closures, which can lead to abrupt braking and sudden lane changes. Most previous research on Connected and Autonomous Vehicles (CAVs) assumes ideal communication conditions, overlooking the effects of message loss and network unreliability. This study presents a comprehensive smart work zone (SWZ) framework that enhances lane-change safety by the integration of both Vehicle-to-Vehicle (V2V) and Vehicle-to-Infrastructure (V2I) communication. Sensor-equipped SWZ barrels and Roadside Units (RSUs) collect and transmit real-time hazard alerts to approaching CAVs, ensuring coverage of critical roadway segments. In this study, a co-simulation framework combining VEINS, OMNeT++, and SUMO is implemented to assess lane-change safety and communication performance under realistic network conditions. Findings indicate that higher Market Penetration Rates (MPRs) of CAVs can lead to improved lane-change safety, with time-to-collision (TTC) values shifting toward safer time ranges. While lower transmission thresholds allow more frequent communication, they contribute to earlier network congestion, whereas higher thresholds maintain efficiency despite increased packet loss at high MPRs. These insights highlight the importance of incorporating realistic communication models when evaluating traffic safety in connected vehicle environments.

Keywords: connected autonomous vehicles; smart work zones; vehicle-to-infrastructure communication; vehicle-to-vehicle communication

check for updates

Academic Editors: Stergios Mavromatis, Yasser Hassan and George Yannis

Received: 11 February 2025
Revised: 30 March 2025
Accepted: 31 March 2025
Published: 4 April 2025

Citation: Nour, M.; Nour, M.; Zaki, M.H. Integrating Vehicle-to-Infrastructure Communication for Safer Lane Changes in Smart Work Zones. *World Electr. Veh. J.* **2025**, *16*, 215. https://doi.org/10.3390/wevj16040215

Copyright: © 2025 by the authors. Published by MDPI on behalf of the World Electric Vehicle Association. Licensee MDPI, Basel, Switzerland. This article is an open access article distributed under the terms and conditions of the Creative Commons Attribution (CC BY) license (https://creativecommons.org/licenses/by/4.0/).

1. Introduction

The rapid expansion of infrastructure renewal projects has led to a growing number of work zones across road networks, with billions of dollars allocated to roadway maintenance and upgrades. While essential, these projects often require lane closures that disrupt daily traffic flow and pose considerable challenges for drivers [1]. Work zones present unique safety risks, particularly during lane-changing maneuvers, as reduced visibility, narrower lanes, and unexpected obstacles can alter driver behavior. These changes in driving patterns heighten the likelihood of collisions and increase overall crash risk [2,3]. Consequently, work zones contribute significantly to both fatal and non-fatal crashes. Mitigating these risks and promoting safer, more efficient traffic movement remains a critical goal in managing the growing frequency and complexity of work zone environments [4].

To address these challenges, emerging technologies in transportation are being explored as potential solutions. Among them, Connected Autonomous Vehicles (CAVs) offer

promising capabilities by enabling vehicles to share real-time information through V2V communication, allowing for coordinated driving behaviors that enhance safety in complex traffic scenarios such as work zones [5]. Through real-time data exchange, CAVs can detect potential hazards earlier and make informed maneuvering decisions—such as initiating early or delayed lane changes, enhancing the lane-level decision making process, adjusting speed to maintain safe headways, or forming tighter platoons to reduce collision risks and improve traffic flow efficiency [6–8]. In environments like work zones, this capability helps prevent sudden lane-change conflicts, reducing both crashes and delays by enabling vehicles to adapt dynamically to rapidly changing traffic conditions [9–11]. Studies exploring the role of CAVs in work zone environments with varying MPRs, showed that the percentage of CAVs significantly affects both traffic flow and safety outcomes [12–14]. However, relying solely on V2V communication poses limitations, as it depends on direct data exchange between vehicles within a restricted range. This can lead to fragmented or delayed information sharing, particularly in high-density traffic or highly dynamic work zone environments. Integrating V2V with V2I communication addresses these gaps by offering a more comprehensive view of the environment, enhancing both coordination and responsiveness across the network [15].

Building on the enhanced situational awareness enabled by V2V and V2I integration, Roadside Units (RSUs) serve as critical infrastructure to further extend communication range and reliability. While V2V communication is limited by its short-range, peer-to-peer structure, RSUs act as fixed intermediaries that broadcast context-specific information—such as events or hazards occurring within a defined geographic area—over a wider range, helping bridge communication gaps in complex environments like work zones [16]. They provide timely updates on traffic conditions, road closures, environmental factors, and potential hazards, ensuring that vehicles receive consistent, area-wide information. This broader coverage improves traffic management and safety by reducing information latency and enhancing coordination across vehicles. In fact, strategically placed RSUs have been shown to reduce communication delays by up to 8 % and minimize data loss, particularly in dense urban settings [17]. Their ability to disseminate accurate, real-time updates has also been linked to reductions in traffic incidents and improved driver compliance with advisories [18]. This makes RSUs especially valuable in work zones, where timely information exchange is essential for maintaining both operational efficiency and roadway safety [19].

Despite these advancements in V2I technology and their proven benefits, a critical need remains to understand how different RSU configurations and communication strategies specifically impact lane-change safety in work zones. The interaction between varying MPRs of CAVs, RSU broadcast parameters, and V2V communication capabilities has not been fully explored in the context of work zone lane-change coordination. Furthermore, the optimal integration of these technologies to maximize safety benefits while maintaining reliable network performance remains an open research question. To address these challenges, this paper evaluates the safety implications of integrating V2I work zone detection with V2V lane-change coordination. The framework uses an RSU that broadcasts work zone location information to approaching CAVs with different transmission reliability thresholds, helping vehicles make informed lane-change decisions. The effectiveness of this approach is analyzed across varying CAV MPRs to understand both safety and communication performance. The framework is evaluated using a co-simulation approach that integrates traffic and communication network simulations through the VEINS, OMNeT++ and SUMO platforms. This enables the analysis of not only traffic flow but also key communication metrics, such as packet loss, under realistic conditions. Safety is assessed using

time gap metrics between vehicles, evaluated through TTC, providing a comprehensive understanding of the system's effectiveness in mitigating lane-change risks in work zones.

The analysis incorporates a co-simulation methodology, exploring the interplay between traffic behavior and communication performance for V2I and V2V communication. Hence, the contributions of this paper are as follows:

1. Evaluates the integration of RSU-based work zone detection with V2V lane-change coordination, analyzing the impact of different transmission reliability thresholds on lane-change safety.
2. Implements a co-simulation framework using VEINS, OMNeT++, and SUMO to assess both safety metrics and communication performance during lane changes in work zone environments.
3. Analyzes the effectiveness of combined V2I/V2V communication for work zone safety across different MPRs, focusing on time-to-collision as a key safety metric.

The rest of this paper is structured as follows: Section 2 summarizes key previous work in the field and highlights the research gaps addressed in this study by providing a detailed review of related work. Section 3 details the simulation framework, including the tools and models used. In Section 4, the simulation results are analyzed and discussed in the context of this study's objectives. Finally, the paper concludes with a summary of the findings, their implications, and potential future work. Through this investigation, this work aims to provide actionable insights into optimizing CAV integration in work zones using V2V and V2I communication. By advancing the understanding of how RSUs and communication errors impact traffic safety in work zones, this study contributes to developing robust strategies for implementing CAV systems that improve overall work zone safety.

2. Related Work

This section reviews the current state of research related to V2I and V2V communication for improving road safety, with a particular emphasis on lane-changing scenarios and smart work zones. The review also highlights key gaps in how communication reliability and network dynamics are incorporated into simulation-based safety assessments.

2.1. V2I and V2V Communication for Traffic Safety

V2I and V2V communication technologies have gained widespread attention for their ability to enhance traffic safety. V2V communication enables direct data sharing between vehicles, while V2I communication adds a broader layer of awareness by leveraging infrastructure such as RSUs. This infrastructure-driven perspective allows vehicles to receive information about upcoming hazards, road conditions, or signal timings beyond their sensor range [20].

Past research demonstrates how V2I communication can augment V2V systems to improve decision-making and reduce collisions. For instance, ref. [21] developed a hazard alert system based on vehicle geo-location and V2V messages. While effective in certain scenarios, its limitation stemmed from a lack of infrastructure input, highlighting the value of V2I communication in expanding situational awareness. Hybrid systems that combine both communication types have shown stronger safety outcomes. The authors of [22] reduced right-angle and near-collisions at unsignalized intersections by 87.5% using early V2I warnings.The authors of [23] applied V2I communication to manage red-light compliance, requiring at least 60% penetration of on-board equipment (OBE) for meaningful impact. The authors of [24] further demonstrated the potential of V2I communication by achieving a 100% collision detection rate in a C-V2I system involving vehicles and pedestrians. However, the study assumed fixed CAM frequencies and simplified traffic

and network conditions, limiting its applicability to real-world scenarios. Other studies explored driver response to infrastructure warnings.The authors of [25] found that audio-based V2I alerts on horizontal curves outperformed text-based and traditional signage in enforcing speed compliance. Similarly, ref. [26] demonstrated that V2I data can extend a CAV's perception at obstructed urban intersections, improving the accuracy and timing of its responses. Collectively, these studies underscore the value of V2I communication in enhancing situational awareness, delivering timely warnings, and supporting more informed and adaptive driving decisions. While the safety benefits of V2I systems are well-documented, many of these efforts rely on idealized communication conditions. This study addresses that gap by incorporating communication imperfections—such as packet loss and limited connectivity—into the safety analysis to more accurately reflect real-world operating environments.

2.2. Lane-Change Safety and Cooperative Communication

Lane-changing maneuvers are among the most safety-critical tasks in driving. Traditional systems relying on vehicle-mounted sensors often lack the ability to anticipate other drivers' intentions, especially in dense traffic [27]. This limitation motivates the need for connected vehicle systems that incorporate V2V and V2I communication for real-time coordination [28,29].

Cut-in detection is one challenge commonly addressed in lane-change safety. Technologies such as Adaptive Cruise Control (ACC) are sometimes unable to accurately predict or respond to sudden merges, leading to unsafe gaps [30]. Adaptive control strategies, such as the Adaptive Fuzzy-PID (AFUPID) controller [31], have been proposed to improve speed regulation and responsiveness, particularly in CV environments. Fuzzy logic control, which is central to AFUPID, is a rule-based approach that effectively handles system uncertainties and nonlinearities. As demonstrated in [32], fuzzy controllers dynamically adjust output responses based on linguistic rule sets and membership functions, allowing for real-time adaptation to varying conditions. This approach enhances stability and responsiveness, which are crucial for maintaining safe vehicle gaps in unpredictable driving scenarios.

Other studies have investigated predictive lane-change models and cooperative planning strategies. The authors of [33] focused on early prediction of surrounding vehicles' behaviors, while [34] applied inverse reinforcement learning to imitate human-like lane-changing decisions shared over Vehicle-to-Everything (V2X) channels. Cooperative trajectory planning that integrates V2I and V2V communication, as demonstrated in [35,36], offers another promising direction, especially when real-time road geometry and obstacle data are shared with CAVs. Some approaches use V2X data to assess lane-change risk or predict incident likelihoods. For example, ref. [18] proposed an incident alert system using RSUs to monitor lane-change behavior and disseminate warnings. Their system, tested using the VEINS simulation platform, led to a 25% reduction in queue size and 20% faster dissipation.

While the studies above highlight the promise of V2I/V2V cooperation, many assume ideal communication conditions. Table 1 summarizes assumptions made in key studies regarding communication reliability and network modeling.

Table 1. Common assumptions in V2V/V2I networking studies.

Citation	Key Assumptions
[24]	Assumes 100% CAV market penetration. Transmission delays are not considered.
[35]	Ideal communication is assumed—no data loss or delay in V2V/V2I links. Full-state vehicle data (velocity, acceleration, jerk, position, etc.) is shared in real time among all vehicles.
[36]	Network delays and packet losses are ignored. Communication architecture between infrastructure and vehicles is not described.
[37]	Traffic flow is simulated using SUMO, but communication modeling is not included.

2.3. V2X Communication in Work Zones

Work zones introduce additional complexity due to lane closures, reduced visibility, and altered traffic dynamics. Several studies have addressed CAV deployment in these contexts. For example, ref. [38] examined late merge strategies, while [13,39] evaluated the effects of varying MPRs on efficiency and safety. Some work has proposed merging and coordination systems using V2X, such as [5,40], but often without detailed modeling of the communication layer. Our study differs by incorporating message reliability and delay into the lane-change decision-making process.

Table 2 summarizes recent studies focused on CAV applications in work zones, highlighting both their contributions and limitations.

Table 2. V2I and CAV applications in smart work zones.

Citation	Summary of Findings
[11]	Introduces a reinforcement learning-based cooperative merge control strategy for highway work zones. Simulation results show improved mobility and safety over traditional early and late merge methods, particularly under heavy traffic conditions.
[14]	Uses agent-based modeling to explore safety impacts of V2V and V2I connectivity in mixed traffic. Varying connectivity levels and flow rates were tested in a four-lane highway work zone.
[15]	Analyzes CAV performance under different traffic demands in work zones. Integration of V2V and V2I communications resulted in a 40% reduction in mean travel time and a 65% increase in capacity.
[18]	Shows that RSUs improve real-time dissemination of road closure and hazard alerts, leading to fewer incidents and better driver compliance with advisories.
[17]	Demonstrates that RSUs can reduce communication delays by up to 8%, emphasizing their importance in enhancing the reliability of V2V and V2I networks.
[41]	Compares trajectory planning methods for CAVs navigating roadwork zones. Use of Smart Traffic Cones (STCs) reduced traffic conflicts by 40% and delays by 3% compared to in-vehicle sensors alone.
Current Study	Proposes a comprehensive smart work zone framework integrating V2I communication and sensor-equipped barrels. Uses a co-simulation platform to assess the impact of communication errors on lane-change safety.

2.4. Simulation Frameworks and Communication Modeling

Most studies assessing connected vehicle safety use traffic-only simulations or assume ideal communication performance. However, real-world conditions involve packet drops, network delays, and congestion. To address this, co-simulation frameworks like VEINS integrate traffic and communication modeling using SUMO and OMNeT++ via the TraCI

interface [42]. Studies such as [43] have demonstrated that communication imperfections significantly impact safety outcomes, particularly in intersection management. Others, like [44], propose network-level enhancements like broadcast suppression to improve message delivery in Vehicular Ad Hoc Networks (VANETs).

Our study leverages VEINS to bridge the gap between traffic behavior and network dynamics. Unlike prior work that assumes error-free connectivity, we incorporate packet delivery ratio and latency into the decision logic for lane-changing maneuvers. By simulating V2V and V2I communication under varying MPRs and communication thresholds, we offer a more realistic and comprehensive safety assessment in smart work zones.

3. V2I Framework for Smart Work Zone Communication Systems

This section presents the developed simulation framework that integrates V2V and V2I communication to enhance safety and traffic flow in SWZs. The system models vehicle behavior in lane closures using a multi-layer communication and traffic co-simulation environment.

At the core of the framework, the RSU determines and broadcasts lane closure alerts to approaching CAVs based on empirically derived PDR distributions rather than modeling the direct barrel-to-RSU communication. Findings from our prior research on BLE reliability in SWZ are incorporated to inform RSU message transmission probabilities [45]. Figure 1 illustrates the communication framework. The closed lane is monitored by BLE-equipped barrels relaying updates to an RSU, which then broadcasts location-related information to incoming vehicles. Meanwhile, CAVs exchange real-time data using V2V communication to coordinate merging and lane-changing maneuvers.

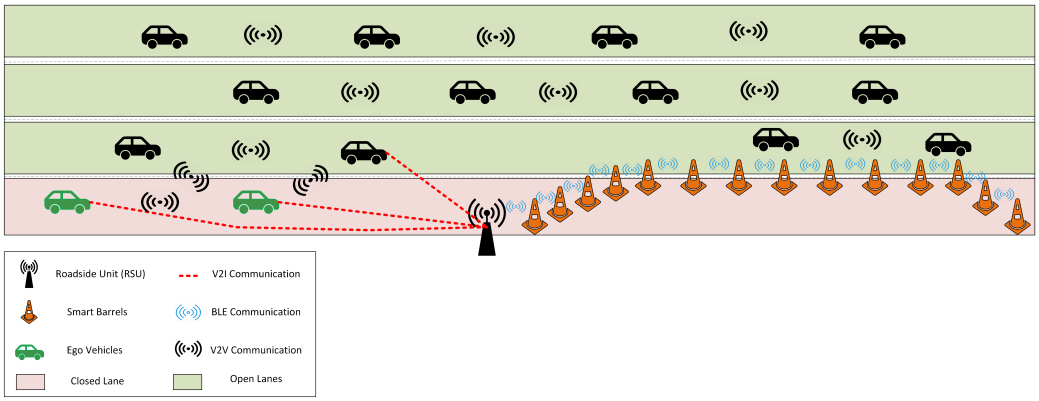


Figure 1. Smart work zone communication framework: An RSU broadcasts lane closure information to CAVs via V2I communication, while smart barrels use BLE to relay updates to the RSU. V2V communication enhances vehicle coordination for safer lane changes.

By integrating empirical communication reliability and traffic micro-simulation, this framework enables a detailed analysis of how network constraints impact vehicle behavior. The following subsections describe the simulation environment, co-simulation architecture, traffic modeling approach, and implementation of realistic V2I communication.

3.1. Simulation Environment and Co-Simulation Framework

This section details the simulation setup and co-simulation architecture used to evaluate CAV behavior and V2I communication reliability in a smart work zone scenario. It outlines the simulation parameters followed by a description of the integrated VEINS-based platform that links traffic and communication models. The goal is to assess how varying connectivity levels and communication performance influence lane-change safety near lane closures.

3.1.1. Simulation Setup

The simulation evaluated various CAV Market Penetration Rates (MPRs) at 10%, 30%, 50%, 70%, and 100%, across different RSU broadcast frequency thresholds of 0.70, 0.85, and 0.95. A 0% MPR scenario was not included, as V2I communication requires at least a minimal level of connectivity among vehicles to operate. The 10% MPR case serves as a practical baseline for assessing system performance under limited connectivity. Each simulation ran for 30 min, including a 5-minute warm-up phase followed by 25 min of data collection. The warm-up period allowed traffic flow to stabilize and reach a steady state, preventing initial transient behavior from skewing results. During this phase, vehicles populated the network and established natural car-following patterns and lane positions. Without this warm-up period, the analysis would include initialization artifacts that do not reflect realistic traffic conditions. To account for stochastic variability, each scenario was repeated five times with different random seeds for both traffic and network simulations. All subsequent analysis is based on the aggregated output across these runs to ensure statistical robustness. The following sections provide a detailed discussion of the traffic data sources, modeling approaches, and calibration process used to align the simulation with real-world conditions.

3.1.2. Co-Simulation Framework

The integrated simulation framework utilizes a co-simulation approach to model both traffic dynamics and CAV communications. The framework, as seen in Figure 2, leverages three key components: SUMO for traffic microsimulation, OMNeT++ for network simulation, and VEINS as the integration middleware. SUMO provides the foundation for modeling realistic vehicle movements with customizable car-following and lane-changing models. Through its TraCI protocol interface, SUMO enables real-time parameter adjustments during simulation, allowing vehicles to adapt based on received communications. The communication aspects are handled by OMNeT++, a discrete event-based network simulator designed for modeling communication protocols. OMNeT++ simulates message transmission between vehicles and infrastructure, accounting for signal propagation, interference, and packet loss. VEINS serves as the middleware that synchronizes the traffic and communication simulations. Acting as a client to SUMO's server, VEINS facilitates bidirectional data exchange: vehicle positions flow from SUMO to OMNeT++, while communication outcomes influence vehicle behaviors in SUMO.

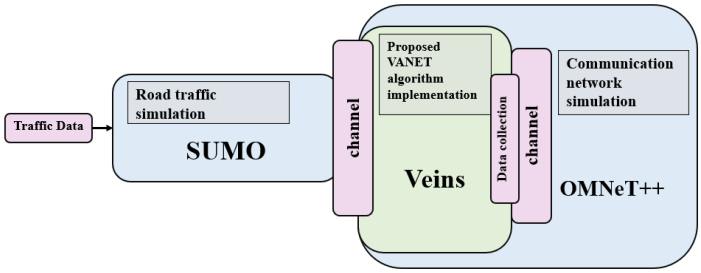


Figure 2. Traffic and communication network co-simulation framework.

This co-simulation approach allows for a realistic assessment of how communication reliability affects lane-change coordination in work zones, providing insights unattainable through isolated traffic or network simulations.

3.2. Traffic Simulation Models

The traffic simulation model is designed to replicate real-world driving behavior while integrating V2V and V2I communication to study their impact. The traffic model is

developed and calibrated using empirical traffic data to ensure realistic vehicle interactions. This section discusses the data sources, traffic modeling approaches, and calibration process used to align simulated vehicle behavior with observed traffic patterns.

3.2.1. Vehicle Modeling in SUMO

For car-following behavior, the Adaptive Cruise Control (ACC) model is applied to both CAVs and human-driven vehicles (HDVs), following the approaches in [46,47]. While HDVs rely solely on ACC for maintaining safe distances, CAVs enhance their responsiveness by integrating V2V communication, allowing real-time traffic adjustments.

Lane-changing maneuvers are governed by SUMO's LC2013 model, which factors in speed control, gap acceptance, and driver cooperation [48]. It classifies lane changes into four distinct categories—strategic, cooperative, tactical, and regulatory—ensuring that vehicles adapt their movements based on observed traffic conditions. Unless explicitly modified, SUMO assumes lane changes occur instantaneously, providing a flexible approach to modeling complex environments such as work zones.

3.2.2. Traffic Simulation Model Development and Calibration

The car-following simulation model was developed and calibrated using real-world traffic data from loop detectors along a four-mile eastbound segment of SR528 in Orlando, Florida, which includes multiple on-ramps and off-ramps (Figure 3). Data were collected during the morning peak on 2 May 2020, to reflect realistic traffic conditions. Speed, volume, and occupancy were recorded at each detector and aggregated into 1-minute intervals to develop and calibrate the traffic network. The work zone setup involved closing a 1 km rightmost lane to simulate a typical lane closure scenario. The RSU was positioned at the start of the work zone closure, where lane restrictions begin. It periodically broadcasted the closure start coordinates to incoming CAVs, ensuring they received advance notice within its 900-meter communication range to initiate safe lane changes.



Figure 3. Simulated segment of the SR528 Highway in Orlando, FL, USA.

The road network was extracted from OpenStreetMap and imported into SUMO. Loop detectors were positioned to match real-world locations obtained from the RITIS database. Traffic flows were then generated based on the volumes and speeds obtained from the traffic data. The ACC model, as discussed earlier, was applied to regulate vehicle behavior based on surrounding traffic conditions. Model parameters were calibrated using observed traffic volume and speed data to ensure accurate simulation results [49].

The calibration process utilized Geoffrey E. Heavers (GEH) statistics and absolute speed difference (ASD) to evaluate the accuracy of simulated traffic volume and speed, respectively. The GEH statistic [50] was calculated using Equation (1):

$$GEH = \sqrt{\frac{2 \times (V_{obs} - V_{sim})^2}{V_{obs} + V_{sim}}} \quad (1)$$

where V_{sim} and V_{obs} represent the simulated and observed traffic volumes. Following calibration standards from [51], a GEH value below 5 is required for at least 85% of the data points. Our results showed that 99% of the data points satisfied this criterion, indicating strong agreement between simulation and field volume data.

Speed accuracy was assessed using the absolute speed difference (ASD), computed as:

$$ASD = |S_{sim} - S_{obs}| \quad (2)$$

where S_{sim} and S_{obs} denote the simulated and observed speeds. To meet calibration requirements, ASD must be under 2.5 m/s for at least 85% of the data. Our simulation achieved this with 86.73% of data points falling within the acceptable range, demonstrating high fidelity in speed reproduction.

Calibration adjustments focused on four primary vehicle behavior parameters: acceleration, deceleration, time headway (τ), and speed factor as seen in Table 3. These parameters were iteratively tuned to minimize discrepancies between simulated and real-world data, ensuring realistic vehicle responses and traffic flow dynamics.

Table 3. SUMO calibration parameters.

Parameter	Default	Range	Calibrated
Acceleration (m/s^2)	2.6	2.6–5.6	4.5
Deceleration (m/s^2)	4.5	4.5–7.5	6.5
Tau (seconds)	1.0	1.0–1.5	1.3
SpeedFactor	normc(1,0.1,0.2,2)	-	normc(0.7,0.05,0.4,0.75)

For lane-changing behavior, SUMO's default politeness factor, gap acceptance thresholds, and speed gain probability were retained, as prior research has validated these parameters [48]. This approach ensures that lane-changing interactions remain realistic while allowing focus on the impact of V2V and V2I communication in traffic dynamics.

3.3. Communication System Implementation

The implementation of a robust communication system is essential for reliable information exchange in SWZs. This section outlines our approach integrating V2V and V2I communication frameworks. The multi-layered architecture ensures connected vehicles receive timely information about lane closures while maintaining system resilience across varying conditions. Our implementation incorporates realistic communication models based on empirical data to accurately represent real-world challenges.

3.3.1. Vehicle-to-Vehicle Communication

At the foundation of the simulated V2V model, the physical-layer network implementation controls how wireless signals propagate between vehicles. The communication system follows a path loss model to simulate signal attenuation based on distance, transmission power, and environmental factors. The received signal power is determined by:

$$P_{recv} = P_{transmit} \times \frac{c^2 d^{-\alpha}}{16\pi^2 f^2} \quad (3)$$

where P_{recv} is the received power, $P_{transmit}$ is the transmission power, d is the distance between sender and receiver, f is the signal frequency, and c is the speed of light. This formulation ensures a realistic simulation of communication effectiveness in varying traffic densities and road conditions [52].

Building upon the physical layer, Dedicated Short-Range Communications (DSRC) using IEEE 802.11p protocol with specific medium access control (MAC) layer settings was implemented (shown in Table 4). The potential for message collisions is mitigated through the CSMA/CA protocol inherent in the 802.11p MAC layer, which uses carrier sensing and random backoff mechanisms to reduce packet contention in shared channels. DSRC

is specifically designed for vehicular environments, offering low-latency, high-reliability communication essential for safety-critical applications.

Table 4. Communication network simulation parameters.

Parameter	Range
Transmission Power	20 mW
Sensitivity	−85 dBm
Transmission range	300 m
Bitrate	6 Mbps
Beacon Frequency	10 Hz

At the application level, CAVs utilize this communication model to exchange essential information such as position, speed, and road conditions. This allows vehicles to maintain situational awareness, assess time gaps, and coordinate lane changes in a cooperative manner. When a CAV receives information from the RSU about the existence of a lane closure, it evaluates real-time information from nearby CAVs to determine a safe lane-change opportunity. The decision-making process involves analyzing time gaps between leading and lagging vehicles in the target lane to ensure smooth and predictable maneuvers, with a total accepted gap of at least 3 s based on typical lead and lag gap thresholds reported in [53].

Time gaps are computed using Equation (4):

$$t_{gap} = \frac{x_i - x_{i-1}}{v_{i-1}} \tag{4}$$

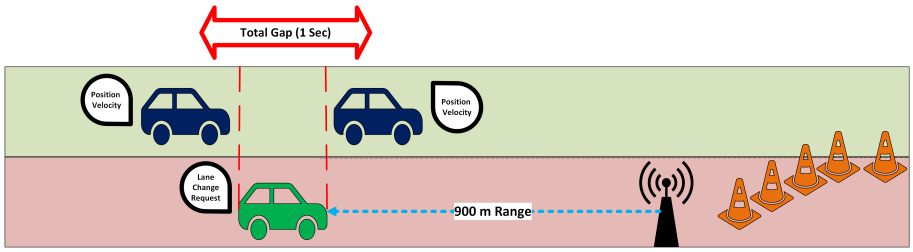
where x_i is the position of the ego vehicle, x_{i-1} is the position of the lag vehicle, and v_{i-1} is the velocity of the lag vehicle.

As illustrated in Figure 4, the cooperative lane-change process relies on V2V communication, where CAVs broadcast their position and velocity data. When a CAV detects an upcoming lane closure, it sends a lane-change request to the lead and lag vehicles in the target lane. The gap between vehicles is then evaluated, and based on this information, the involved vehicles adjust their speeds accordingly to create a safe lane-changing opportunity. A successful merge would be a completed lane-change maneuver in which a CAV safely transitions into the target lane without violating critical safety constraints, such as minimum TTC thresholds. The maneuver must occur without abrupt braking, erratic behavior, or failed coordination with surrounding vehicles. A successful merge reflects a smooth and safe integration into traffic, enabled by cooperative V2V communication with lead and lag vehicles.

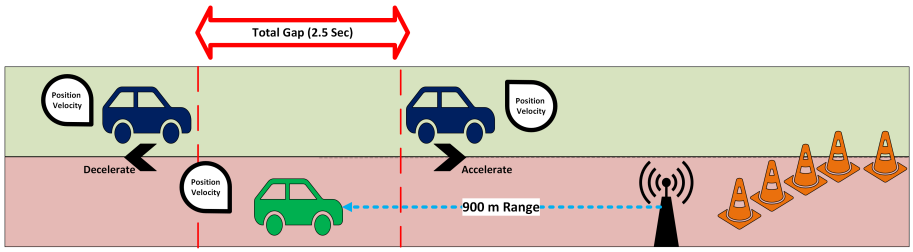
By integrating both lower-layer network dynamics and application-level coordination, this communication framework enhances the safety and efficiency of cooperative lane changes in complex traffic scenarios. The continuous exchange of position and speed data allows CAVs to make informed decisions, reducing abrupt lane changes and improving overall traffic flow.

A key challenge in such environments is accommodating mixed traffic, where both CAVs and HDVs coexist. To accurately model these interactions, the simulation accounts for varying traffic compositions and vehicle behaviors. CAVs prioritize V2V communication to negotiate gaps when both the leading and following vehicles are connected. Otherwise, they revert to conventional car-following and gap acceptance principles to ensure safe maneuvering. This adaptive approach enables dynamic coordination while maintaining realistic lane-changing behavior in diverse traffic conditions. Building on this, the data dissemination algorithm governs when a CAV should initiate a lane change. Once a

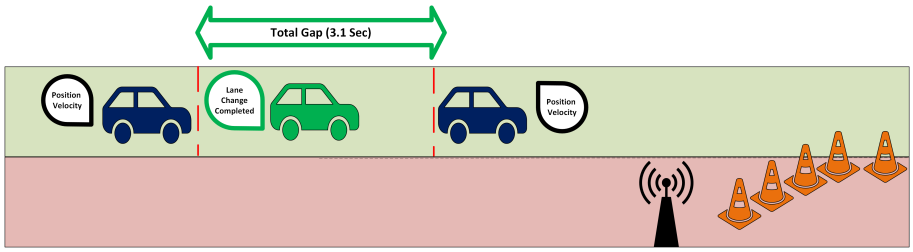
decision is made, SUMO's default lane-changing model executes the maneuver, ensuring consistency with the overall traffic dynamics.



(**a**) Initial lane-change request with a total gap of 1 second.



(**b**) Vehicles adjusting speed to facilitate lane change with a total gap of 2.5 seconds.



(**c**) Lane change successfully completed with a total gap of 3.1 seconds.

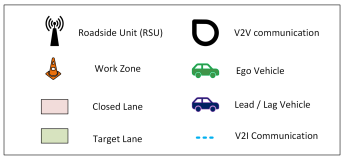


Figure 4. Illustration of the V2V communication process for cooperative lane change in a work zone scenario. The sequence shows how CAVs negotiate a lane change by exchanging position and velocity information and adjusting speeds accordingly. (**a**) The ego vehicle (green) initiates a lane-change request with an initial gap of 1 s. (**b**) CAVs in the target lane receive this information and start adjusting their speeds, with the lead vehicle accelerating and the lag vehicle decelerating to create a larger gap. (**c**) Once a safe gap of 3.1 s is achieved, the ego vehicle successfully completes the lane change.

3.3.2. Vehicle-to-Infrastructure Communication

The communication framework for the SWZ leverages a barrel-to-RSU architecture developed in our previous research on BLE-based deployments in SWZs [45]. In that work, Bluetooth Low Energy (BLE) was selected for this application due to its cost-effectiveness, low power consumption, minimal infrastructure requirements, and sufficient communication range when used with a relay-based approach. These characteristics make BLE particularly well-suited for temporary, battery-powered deployments such as work zones. To overcome BLE's inherent range and interference limitations—especially in dense traffic environments—we incorporated the clustering-based relay node selection algorithm developed in our earlier work. This algorithm strategically selects relay barrels based on spatial

location and network load to optimize multi-hop message propagation. While multi-hop relaying introduces some latency, the proposed approach consistently maintained packet delivery ratios above 80%, effectively extending BLE's operational coverage across the SWZ barrels while preserving energy efficiency. In this study, rather than explicitly modeling the barrel-to-RSU communication, we adopted an empirical Cumulative Distribution Function (CDF) derived from our prior simulations to realistically represent message delivery within the SWZ network and reduce the overall simulation complexity.

Building on this empirical modeling approach, the RSU processes incoming barrel data using a threshold-based transmission mechanism. Thresholds (θ) of 0.70, 0.85, 0.90 were applied to determine whether a message should be broadcast. These decisions are informed by sampling from the previously derived PDR distribution, with transmissions occurring only when the sampled values exceed the selected threshold. This mechanism is described in more detail in the subsequent sections.

To support this framework, the work zone is configured with a single RSU strategically placed at the beginning of the 1 km closure. Positioned just before the taper, this RSU acts as a centralized communication hub for the system with a communication range of 900 m. This single-unit design reflects practical deployment considerations, balancing effective coverage with minimal infrastructure requirements.

Once the barrel data are aggregated, the RSU broadcasts coordinates of the lane closure's starting point to the incoming vehicles. The key parameters for RSU communication were configured as shown in Table 5.

Table 5. RSU communication parameters.

Parameter	Value
Communication Range	900 m
Transmission Power	20 mW
Receiver Sensitivity	−95 dBm
Beacon Interval	1 s
Message Content	Work zone starting coordinates

While the current implementation focuses on location dissemination, the RSU framework is extensible and can be adapted to include additional data such as total work zone length, number of closed lanes, recommended speed limits, or merging guidance in future deployments.

3.4. Implementing Realistic Communication Models

To create a realistic model of communication in SWZs while maintaining computational efficiency, this study employs an empirical approach that captures the reliability characteristics of barrel-to-RSU communication. Rather than conducting detailed simulation of BLE network protocols, which would be computationally intensive, we leverage empirical data from our previous research on SWZ barrels [45]. This approach allows us to incorporate real-world communication behavior while focusing on the effects of reliability on safety outcomes.

3.4.1. Simulating Communication Reliability with Empirical PDR Distributions

To incorporate realistic work zone barrel communication performance into the simulation, we first define the Packet Delivery Ratio (PDR) as the ratio of successfully received packets to the total number of packets transmitted:

$$PDR = \frac{N_{received}}{N_{sent}} \tag{5}$$

To represent variability in communication performance, empirical PDR distributions are transformed into a Cumulative Distribution Function (CDF). The CDF enables estimation of the probability of achieving different levels of reliability without simulating the full BLE network stack. It is defined as:

$$F(PDR) = P(\text{PDR} \leq x) \tag{6}$$

where $F(PDR)$ denotes the probability that the packet delivery ratio is less than or equal to a given value x.

The inverse transform sampling method generates realistic PDR values directly from this empirical distribution. First, a uniform random number is generated within the range $[0, 1]$:

$$U \sim Uniform(0, 1) \tag{7}$$

The corresponding PDR value is then determined using the inverse CDF:

$$PDR = F^{-1}(U) \tag{8}$$

This approach ensures that simulated PDR values statistically match the empirical distribution rather than relying on arbitrary fixed assumptions. The inverse sampling process is visualized in Figure 5, where uniform random values are mapped to corresponding PDR values.

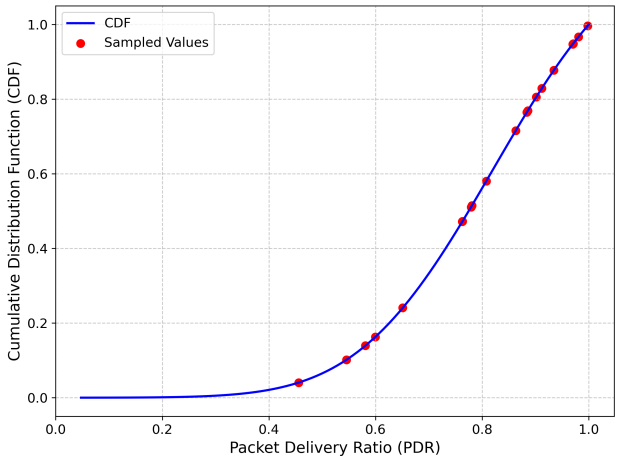


Figure 5. Empirical CDF of SWZ barrel PDR with sampled values using inverse transform sampling.

Message transmission decisions are conditioned on a predefined PDR threshold (θ), which we selected as 0.70, 0.85, and 0.95. The probability of sending a message is determined using:

$$P(Send \mid \theta) = P(PDR \geq \theta) = 1 - CDF(\theta) \tag{9}$$

The selection of these three threshold values provides a comprehensive spread across the reliability spectrum, enabling systematic evaluation of the framework under varying reliability constraints. The 0.70 threshold represents a more permissive approach where some message loss is tolerable, 0.85 represents a balanced middle ground, and 0.95 enforces high-reliability communications approaching guaranteed delivery. This parameter selection allows for a thorough analysis of how different reliability requirements affect both safety outcomes and network performance metrics, investigating the trade-offs between communication frequency and reliability in V2I systems operating in SWZs.

3.4.2. RSU Communication Algorithm

To integrate this process within the simulation, the RSU employs a protocol that uses the above explained process to determine whether to broadcast the location of the work zone to nearby vehicles.

Figure 6 presents the full workflow of this empirical modeling approach. It begins with BLE simulation data, which are transformed into a PDR distribution. The RSU then samples from this distribution and applies a threshold comparison to decide on message transmission.

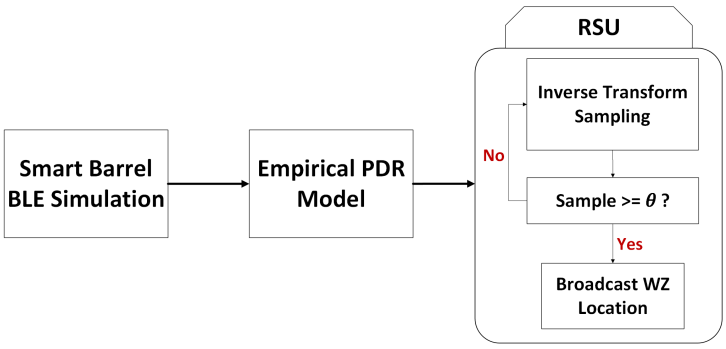


Figure 6. Workflow of the empirical communication modeling approach.

Algorithm 1 operationalizes this process. At each time step, the RSU loads the empirical distribution, samples a PDR value, and compares it to the selected threshold. If the condition is met, a message is broadcast to all CAVs within range. This approach allows the simulation to evaluate how different levels of communication reliability affect safety-critical decision-making across varying CAV penetration rates. This integrated framework captures the interaction between V2I and V2V communication, focusing on how network reliability influences the dissemination of safety information and the success of cooperative maneuvers in work zones. By modeling communication and traffic jointly, this study offers a realistic, data-driven assessment of V2X system performance.

Algorithm 1: RSU Communication Protocol with PDR Inverse Sampling

Data: PDR thresholds $\theta \in \{0.70, 0.85, 0.95\}$, RSU Communication range $R \in \{900m\}$, Market penetration rates $MPR \in \{10\%, 30\%, 50\%, 70\%, 100\%\}$

Initialization: Load empirical PDR distribution $F^{-1}(x)$ from barrel data;
while *simulation running* **do**
  PDR Sampling: Draw $U \sim \text{Uniform}(0, 1)$ and compute $PDR \leftarrow F^{-1}(U)$;
  if $PDR \geq \theta$ **then**
    Message Transmission: for *each CAV i within range R* **do**
      Transmit safety message to CAV i;
    end
  end
  Record Results: Store vehicle trajectories and communication performance metrics;
end

4. Results

In the next subsections, safety and communication metrics are analyzed to understand their impact on each other, highlighting how message reliability influences lane-change safety in the work zone environment.

4.1. Traffic Analysis

To evaluate traffic safety across the simulated scenarios, this study uses time-to-collision (TTC) as the primary surrogate safety measure. TTC quantifies the temporal proximity to a potential collision between consecutive vehicles, defined as the time required for two vehicles to collide if they maintain their current speeds and trajectories [54]. As shown in Equation (10), TTC is calculated using the relative positions, lengths, and velocities of vehicle pairs, with lower values indicating higher collision risk [55].

$$TTC = \frac{x_{i-1}(t) - x_i(t) - l_{i-1}}{v_i(t) - v_{i-1}(t)} \tag{10}$$

where x_{i-1} and v_{i-1} represent the position and velocity of the leading vehicle, while x_i and v_i denote the position and velocity of the following vehicle. For this analysis, interactions with TTC values below 3 s were classified as hazardous. This threshold has been established in prior research [56] as a benchmark to distinguish between safe and high-risk traffic events. Accordingly, the number of instances where TTC falls below this critical threshold was recorded for safety evaluation.

The safety performance across different parameter combinations is visualized through probability density distributions of TTC values. Figures 7–9 present these distributions for various MPRs at transmission thresholds of 0.70, 0.85 and 0.95, respectively. The following analysis examines how increasing MPR affects vehicle interactions in the work zone environment.

At 10% MPR, the TTC distribution exhibits a peak near 0.5 s, indicating frequent close-following situations, which pose a higher safety risk. As MPR increases to 30–100%, the distributions shift towards longer TTC values, signifying safer vehicle spacing. Specifically, at 70–100% MPR, there is a noticeable increase in probability density within the 2.0–3.0 s range, suggesting improved safety margins and better vehicle coordination.

From a risk assessment perspective, the high-risk region (TTC < 1.0 s) shows higher probability densities at lower MPRs, indicating frequent near-collision scenarios. The moderate-risk region (TTC between 1.0 s and 2.0 s) demonstrates a more balanced distribution across different MPRs. In contrast, the safer region (TTC > 2.0 s) exhibits increased probability density at higher MPRs, reinforcing the trend of improved safety with greater connectivity.

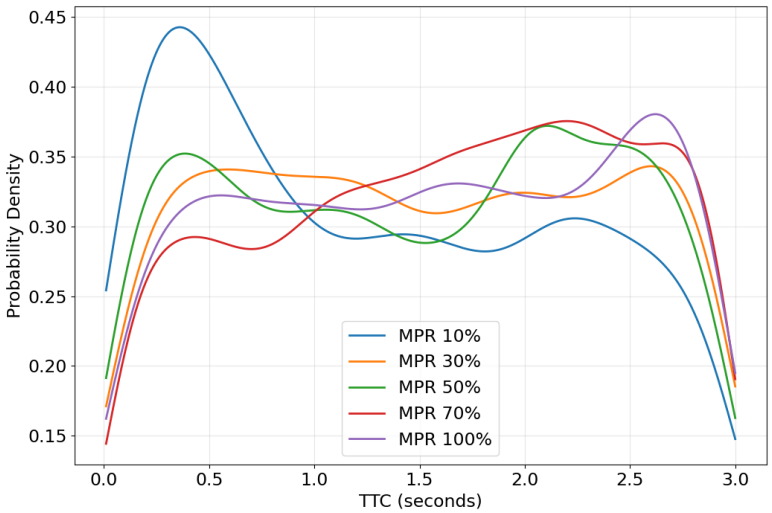


Figure 7. TTC probability density distribution for different MPRs under PDR threshold = 0.70.

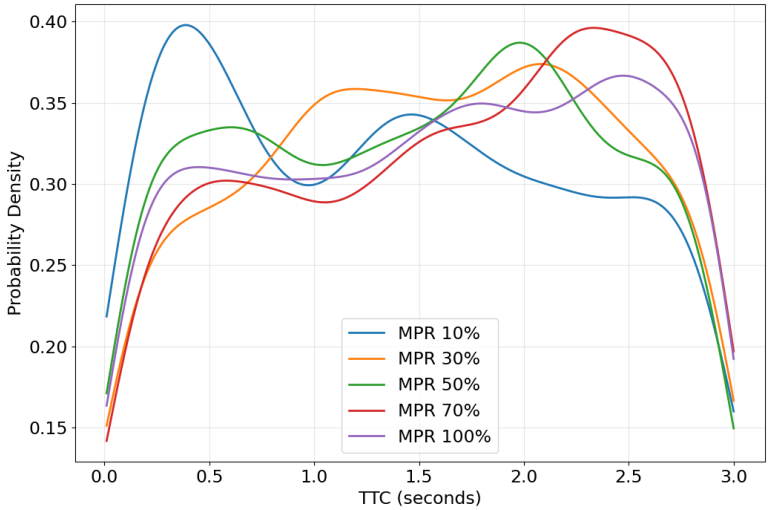


Figure 8. TTC probability density distribution for different MPRs under PDR threshold = 0.85.

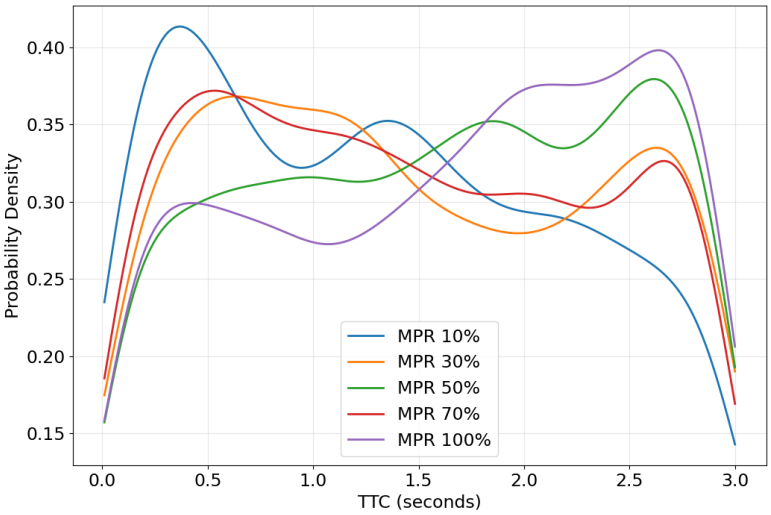


Figure 9. TTC probability density distribution for different MPRs under PDR threshold = 0.95.

Next, the impact of different PDR thresholds is discussed ($\theta = 0.70, 0.85, 0.95$) on the TTC distribution for varying MPRs, as illustrated in Figures 7–9. This analysis highlights the trade-offs between communication reliability from the RSU perspective and safety performance. For the low threshold ($\theta = 0.70$), the system transmits messages most frequently due to the lower reliability requirement. This results in good overall safety performance, particularly at higher MPRs (70–100%), where the distributions show greater density in the safer TTC regions. The findings suggest that even with a more relaxed reliability constraint, the system can maintain safety benefits through increased connectivity. At the medium threshold ($\theta = 0.85$), message transmission becomes more selective, leading to a slightly broader spread in TTC values. The distributions still maintain good safety performance at higher MPRs, but the transition between lower and higher MPRs appears more gradual, reflecting a balance between reliability and communication frequency. The high threshold ($\theta = 0.95$) enforces the strictest reliability requirement, allowing only the most reliable messages to be transmitted. This results in more pronounced differences between MPR levels, with lower MPRs (10–30%) exhibiting higher density in critical TTC regions. While higher MPRs still achieve safety benefits, the distributions show more variation, indicating a greater dependency on connectivity to compensate for the reduced message frequency.

Higher thresholds result in fewer but more reliable messages, while lower thresholds allow more frequent communication with potentially lower reliability. Across all thresholds, safety improves with increasing MPRs, but the highest threshold ($\theta = 0.95$) shows the most distinct differences between MPR levels. Even under the strictest reliability requirement, the system maintains safety benefits at higher MPRs, while the lowest threshold still provides noticeable improvements as connectivity increases. This analysis suggests that the V2I system remains robust across different reliability requirements, with the choice of θ representing a balance between communication frequency and reliability.

The statistical analysis of TTC distributions reveals significant safety improvements with increasing MPRs across all transmission thresholds (Table 6). One-way ANOVA tests yielded highly significant results ($p < 0.0001$) for all thresholds, confirming that the observed differences in TTC distributions are not due to random variation. The Tukey HSD post hoc analysis showed that the lowest MPR (10%) consistently produced the smallest mean TTC values (highest risk), with significantly higher TTC values observed at higher MPRs. The largest improvements were observed with the 95% threshold, where the 100% MPR condition demonstrated a 0.247-s increase in mean TTC compared to the 10% MPR condition. Notably, at the 70% and 85% thresholds, the 70% MPR showed the best performance, while at the 95% threshold, the 100% MPR yielded optimal results.

Table 6. Statistical analysis of TTC distributions across MPRs.

Transmission Threshold	ANOVA F-Value	*p*-Value	Key Pairwise Comparisons (Tukey HSD)
70%	25.26	<0.0001	10% vs. 70%: 0.233 s diff ($p < 0.001$) 50% vs. 70%: 0.088 s diff ($p < 0.001$) 10% vs. 100%: 0.199 s diff ($p < 0.001$)
85%	14.48	<0.0001	10% vs. 70%: 0.193 s diff ($p < 0.001$) 50% vs. 70%: 0.109 s diff ($p < 0.001$) 50% vs. 100%: 0.062 s diff ($p = 0.019$)
95%	31.97	<0.0001	10% vs. 100%: 0.247 s diff ($p < 0.001$) 30% vs. 100%: 0.132 s diff ($p < 0.001$) 70% vs. 100%: 0.154 s diff ($p < 0.001$)

To address the relationship between V2I communications and traffic operations, this study formally quantifies merge success rates across different simulation scenarios. Merge success rate is defined as the percentage of vehicles that successfully complete their initiated lane changes, measured by tracking vehicles that signal intention to change lanes and subsequently confirm completion of the maneuver. When lane changes are attempted but none are completed, the success rate is 0%. Scenarios where no lane changes are attempted are excluded from the analysis. Table 7 presents the merge success rates across different transmission thresholds and MPRs, revealing consistently high success rates (above 90% in most scenarios) despite varying traffic densities.

The total number of merge attempts increases with higher MPRs, from as few as 7 attempts at 30% MPR to over 100 attempts at 100% MPR, reflecting the greater interaction opportunities in traffic environments with higher MPR. The influence of the 85% threshold demonstrates near-perfect success rates (100%) at lower MPRs (10–50%), suggesting that this middle threshold provides an optimal balance between communication reliability and merge coordination effectiveness. Furthermore, at higher MPRs (70–100%), a slight decrease in success rates is observed across all thresholds, though all remain above 90%. This subtle reduction aligns with the increased network congestion observed in the communication analysis, which will be discussed in the upcoming section. Despite the slight decrease in merge success rates at higher MPRs, the overall high success rates (exceeding 90% even

in the most congested scenarios) demonstrate the operational resilience of the proposed V2I framework in facilitating work zone merges across varying traffic conditions and communication reliability.

Table 7. Merge success rates across different thresholds and MPRs.

Transmission Threshold	MPR	Success Rate (%)	Std Dev (%)	Total Attempts
70%	30%	93.33	13.33	16
	50%	96.00	8.00	29
	70%	90.76	5.86	73
	100%	92.19	4.59	91
85%	10%	100.00	0.00	1
	30%	100.00	0.00	18
	50%	100.00	0.00	26
	70%	92.50	10.00	41
	100%	95.85	3.74	108
95%	30%	100.00	0.00	7
	50%	91.36	10.79	27
	70%	95.89	5.64	48
	100%	91.47	7.21	80

4.2. Communication Analysis

The communication analysis examined network performance metrics to evaluate the effectiveness of the V2I framework under varying MPRs and transmission thresholds. Packet loss was calculated to evaluate network performance, with a focus on control messages which are used by CAVs to coordinate lane-change maneuvers.

Packet loss was calculated as the number of control packets that were sent but not successfully received. For each run, the total number of control packets sent and received was extracted, and the packet loss was computed using Equation (11):

$$PacketLoss = \frac{(P_{sent} - P_{received})}{P_{sent}} \tag{11}$$

where P_{sent} is the total number of control packets sent, and $P_{received}$ is the total number of control packets successfully received.

Figure 10 presents the relationship between average packet loss and MPR across different RSU broadcast frequency thresholds (70%, 85%, and 95%). In the low MPR range (10–30%), packet loss remains minimal across all thresholds, aligning with the observed *TTC* distributions that demonstrated clear safety patterns. This indicates that even with a limited number of connected vehicles, the successfully transmitted messages are sufficient to maintain system functionality without network congestion.

As MPR increases to the medium range (40–60%), packet loss begins to rise, particularly for the 70% threshold. Despite this, safety metrics in the *TTC* distributions continued to improve, suggesting that the system remains resilient. Even with moderate packet loss, successful communications are frequent enough to uphold safety benefits. In the high MPR range (70–100%), packet loss increases sharply across all thresholds. However, *TTC* distributions still showed the best safety performance in this range, highlighting that despite higher packet loss, the increased number of connected vehicles ensures that successful message transmissions occur frequently enough to maintain safety benefits. Comparing thresholds, the 70% threshold exhibits an earlier onset of packet loss but a more gradual rise, whereas the 85% and 95% thresholds show steeper increases at high MPRs. Nevertheless, all thresholds maintained safety advantages, reinforcing the system's robustness. The results

indicate that while higher MPRs introduce network congestion challenges, the trade-off between communication performance and safety outcomes remains manageable.

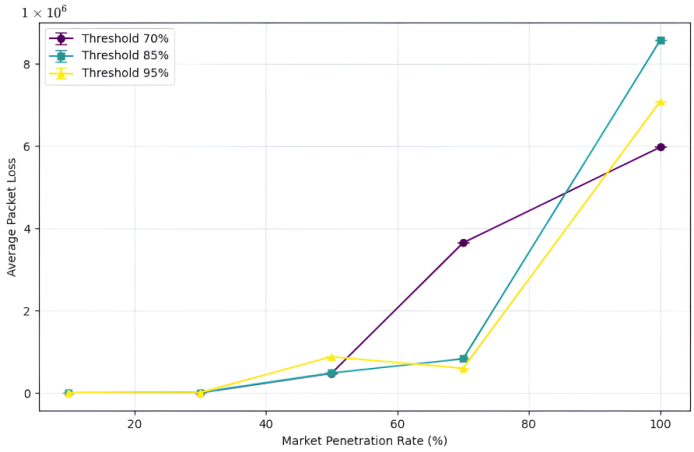


Figure 10. Average packet loss across MPR for different thresholds and ranges.

Channel Busy Ratio (CBR) quantifies the proportion of time that the communication channel is detected as occupied during the observation period. For each simulation run, the total busy time and total observation time were recorded, and the CBR was computed using Equation (12):

$$CBR = \frac{T_{busy}}{T_{total}} \times 100\% \tag{12}$$

where T_{busy} is the cumulative time the channel was detected as busy (occupied by transmissions), and T_{total} is the total duration of the observation period. This metric provides a direct measure of network congestion in the vehicular communication system, reflecting how increasing traffic density affects the availability of the shared wireless medium.

Figure 11 reveals important insights about network congestion in V2V and V2I communication systems.

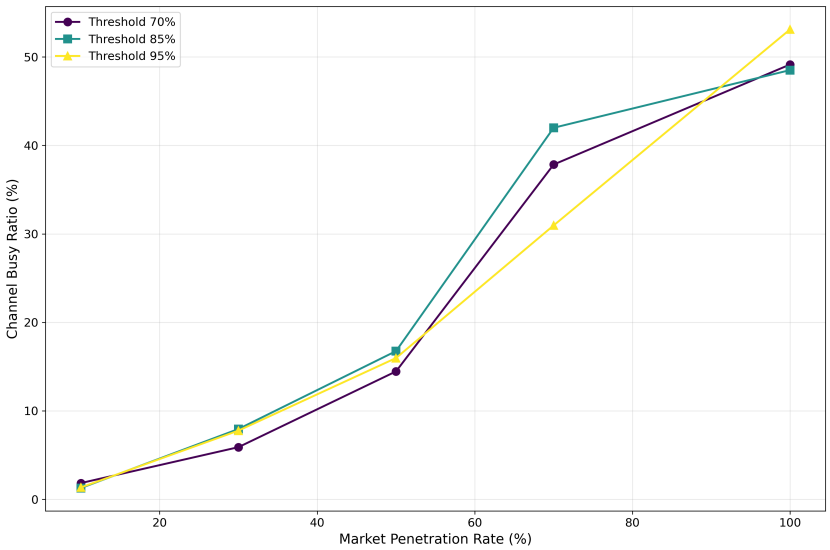


Figure 11. CBR vs MPR comparison across the different thresholds.

As the percentage of CVs increases from 10% to 100%, channel utilization rises substantially across all threshold settings (70%, 85%, and 95%), indicating increasing network congestion. At low penetration rates (10–30%), all thresholds perform similarly with mini-

mal channel occupation. However, at moderate penetration (50–70%), the 95% threshold demonstrates better congestion management compared to lower thresholds. Notably, at 70% MPR, the 85% threshold reaches approximately 42% channel utilization while the 95% threshold maintains a lower 31% utilization. This suggests that higher reliability requirements can paradoxically reduce overall channel congestion by limiting unnecessary transmissions. At full market penetration (100%), all thresholds converge to similar CBR values (49–53%), indicating that threshold selection becomes less impactful when the network is saturated with connected vehicles. These findings highlight the importance of adaptive threshold strategies that respond to varying traffic densities and connected vehicle penetration rates.

4.3. Optimal System Configuration

The results demonstrate that the proposed system effectively enhances safety, particularly at higher MPRs. The TTC distributions indicate a clear shift toward safer time ranges (2.0–3.0 s) as MPR increases, with noticeable safety benefits even at just 10% MPR. Optimal safety performance is observed within the 70–100% MPR range, reinforcing the potential of V2I-assisted lane-change coordination in work zones.

From a network performance perspective, a trade-off exists between message reliability and network load. Lower thresholds (70%) allow more frequent communication but lead to earlier congestion, while higher thresholds (95%) enforce stricter message filtering while maintaining effectiveness. Despite a significant increase in packet loss at high MPRs, safety benefits persist, demonstrating the system's robustness. The system's reliability across different thresholds supports its viability for early deployment, even at low MPR (10–30%). This suggests that implementation can begin before widespread V2V adoption, providing a foundation for gradual technology integration. Additionally, scalability considerations indicate that while the system remains effective under increasing network load, congestion management strategies become essential at higher MPRs. For early-stage deployments, lower thresholds (70%) may be sufficient, focusing on basic work zone detection and essential safety messaging. As the system matures, higher thresholds (85–95%) should be considered to optimize network performance while ensuring reliable communication. Implementing congestion control mechanisms at high MPRs can further balance message frequency and reliability requirements. Overall, these findings suggest that V2I integration for work zone detection effectively complements V2V-based lane-change coordination, providing consistent safety benefits while maintaining manageable network trade-offs across various deployment scenarios.

The merge success rate and CBR analysis further validate the system's effectiveness across varying deployment scenarios. Merge success rates consistently exceed 90% across all configurations, with the 85% threshold demonstrating optimal performance at lower MPRs (perfect 100% success rates at 10–50% MPR). This indicates that a mid-range threshold provides an ideal balance for early deployments. The CBR analysis reveals that at low penetration rates (10–30%), all thresholds maintain minimal channel occupation (1–8%), enabling reliable communications. As the MPR increases, the 95% threshold demonstrates superior congestion management at moderate penetration rates, maintaining lower channel utilization (31% at 70% MPR) compared to other thresholds. However, at full market penetration (100%), all thresholds converge to similar CBR values (49–53%), suggesting that in dense deployment scenarios, additional congestion control mechanisms may become necessary regardless of threshold selection. These findings support a phased deployment approach, beginning with lower thresholds (70–85%) in early stages when MPR is low, then transitioning to higher thresholds (95%) as connectivity increases, eventually incorporating dedicated congestion control mechanisms for widespread deployment.

5. Conclusions

This study presents a comprehensive evaluation of a combined V2I/V2V communication framework for improving lane-change safety in work zones. By integrating probabilistic message transmission mechanisms and assessing their impact across varying MPRs, the findings contribute to both methodological advancements and practical system design considerations. The results indicate that the proposed system significantly enhances lane-change safety in work zones, especially at higher MPRs. As the MPR increases, the TTC distributions shift toward safer time ranges (2.0–3.0 s). The highest safety performance is observed within the 70–100% MPR range, highlighting the effectiveness of V2I-assisted lane-change coordination. In terms of network performance, a balance must be maintained between message reliability and network load. Lower thresholds (0.70) support more frequent communication but lead to earlier congestion, while higher thresholds (0.95) enforce stricter message filtering while still maintaining safety benefits. Despite an increase in packet loss at high MPRs, the system remains effective, demonstrating resilience to network limitations. The proposed methodology successfully demonstrates an approach for evaluating safety-network performance trade-offs in connected vehicle environments. This study establishes a framework for assessing system performance across different penetration rates, offering a structured method for analyzing the interplay between communication reliability and safety outcomes. These findings can inform future research into optimizing V2I and V2V integration for enhanced traffic management and safety applications.

This study focused on work zone lane-change safety, but the proposed framework can be extended to other V2I/V2V applications such as intersection management, emergency vehicle coordination, and coordinated merging assistance. RSUs can also be enhanced to provide additional functionalities beyond lane closure notifications, including speed advisories, real-time routing updates, and proactive merging guidance. Network congestion at high MPRs remains a challenge, and future work will explore adaptive transmission strategies to improve communication efficiency. Potential approaches include using CBR monitoring to regulate transmission frequency, message prioritization frameworks for safety-critical information, and adaptive transmission power control based on local traffic density. To provide a more comprehensive evaluation of traffic safety, future work will expand beyond TTC and incorporate alternative surrogate measures such as Post-Encroachment Time (PET) and Deceleration Rate to Avoid Collision (DRAC). Additionally, conflict severity classification and crash probability models will be explored to assess potential crash risks under different connectivity scenarios. Currently, CAVs in the simulation are modeled as fully compliant, following prescribed acceleration, deceleration, and lane-change commands. Future work will introduce mixed traffic conditions where connected human-driven vehicles exhibit varying levels of compliance and reaction variability. Furthermore, the fixed PDR thresholds (0.70, 0.85, 0.95) will be expanded to include dynamic thresholding mechanisms that adapt based on network congestion and real-time traffic conditions. To further assess system robustness, future research will examine worst-case scenarios such as high network latency, packet loss, and low CAV penetration rates, which may limit the effectiveness of cooperative lane-changing strategies. Additionally, the impact of aggressive human-driven vehicles on CAV behavior will be analyzed, and fallback mechanisms will be developed to handle disruptions in cooperative maneuvers.

By addressing these challenges, future iterations of this framework aim to enhance system adaptability, broaden its applicability, and ensure safer and more reliable lane-changing in complex traffic environments.

Overall, this study establishes baseline performance metrics for similar V2I/V2V systems, offering insights into scalability, network capacity, and safety performance. The results underscore the importance of balancing communication reliability with network

efficiency, paving the way for future research and deployment strategies in connected vehicle environments.

Author Contributions: Study conception and design: M.N. (Mariam Nour) and M.H.Z.; simulation: M.N. (Mariam Nour) and M.N. (Mayar Nour); analysis and interpretation of results: M.N. (Mariam Nour); draft manuscript preparation: M.N. (Mariam Nour), M.N. (Mayar Nour) and M.H.Z. All authors have read and agreed to the published version of the manuscript.

Funding: This research received no external funding.

Data Availability Statement: The original contributions presented in this study are included in the article. Further inquiries can be directed to the corresponding author.

Conflicts of Interest: The authors declare no conflict of interest.

Abbreviations

The following abbreviations are used in this manuscript:

ITSs	Intelligent Transportation Systems
CAV	Connected Autonomous Vehicle
ACC	Adaptive Cruise Control
VANETs	Vehicular Ad Hoc Networks
HDV	Human-Driven Vehicle
SWZ	Smart Work Zone
RSU	Roadside Unit
V2V	Vehicle-to-Vehicle
V2I	Vehicle-to-Infrastructure
V2X	Vehicle-to-Everything
MPR	Market Penetration Rate
PDR	Packet Delivery Ratio
TTC	Time-to-Collision

References

1. Mashhadi, A.H.; Farhadmanesh, M.; Rashidi, A.; Marković, N. Review of methods for estimating construction work zone capacity. *Transp. Res. Rec.* **2021**, *2675*, 382–397.
2. Qi, Y.; Zhao, Q. Safety impacts of signalized lane merge control at highway work zones. *Transp. Plan. Technol.* **2017**, *40*, 577–591. [CrossRef]
3. Gan, X.; Weng, J.; Li, W.; Han, M. Spatial-temporal varying coefficient model for lane-changing behavior in work zone merging areas. *J. Transp. Saf. Secur.* **2022**, *14*, 949–972. [CrossRef]
4. La Torre, F.; Domenichini, L.; Nocentini, A. Effects of stationary work zones on motorway crashes. *Saf. Sci.* **2017**, *92*, 148–159.
5. Hussain, M.; Glaser, S.; Larue, G.S.; Dehkordi, S.G.; Masoud, M. A Cooperative Lane-Change Behaviour Evaluation for Connected and Autonomous Vehicles in Road Work Zones Environments. *IEEE Trans. Intell. Veh.* **2024**, 1–25. . [CrossRef]
6. Wu, W.; Sun, R.; Ni, A.; Liang, Z.; Jia, H. Simulation and evaluation of speed and lane-changing advisory of CAVS at work zones in heterogeneous traffic flow. *Int. J. Mod. Phys. B* **2020**, *34*, 2050201.
7. Nour, M.; Farid, Y.; Xu, L.; Lee, C.; Oguchi, K. Lane Planning of Connected Autonomous Vehicles using a Graph Representation of Road Contents. In Proceedings of the 2024 IEEE International Conference on Smart Mobility (SM), IEEE, Niagara Falls, ON, Canada, 16–18 September 2024; pp. 230–235.
8. Nour, M.; Zaki, M.H. Toward Formalization and Monitoring of Microscopic Traffic Parameters Using Temporal Logic. *Transp. Res. Rec.* **2023**, *2677*, 625–638.
9. Zhu, T.; Li, X.; Fan, W.; Wang, C.; Liu, H.; Zhao, R. Trajectory Optimization of CAVs in Freeway Work Zone considering Car-Following Behaviors Using Online Multiagent Reinforcement Learning. *J. Adv. Transp.* **2021**, *2021*, 9805560.
10. Ma, W.; Chen, B.; Yu, C.; Qi, X. Trajectory planning for connected and autonomous vehicles at freeway work zones under mixed traffic environment. *Transp. Res. Rec.* **2022**, *2676*, 207–219. [CrossRef]
11. Ren, T.; Xie, Y.; Jiang, L. Cooperative highway work zone merge control based on reinforcement learning in a connected and automated environment. *Transp. Res. Rec.* **2020**, *2674*, 363–374.

12. Kim, S.; Kim, Y.; Kim, Y.; Lee, C. PID-Based Freeway Work Zone Merge Control with Traffic State Prediction under Mixed Traffic Flow of Connected Automated Vehicles and Manual Vehicles. *J. Adv. Transp.* **2024**, *2024*, 5554608. [CrossRef]
13. Genders, W.; Razavi, S.N. Impact of connected vehicle on work zone network safety through dynamic route guidance. *J. Comput. Civ. Eng.* **2016**, *30*, 04015020. [CrossRef]
14. Abdulsattar, H.; Mostafizi, A.; Wang, H. Surrogate safety assessment of work zone rear-end collisions in a connected vehicle environment: Agent-based modeling framework. *J. Transp. Eng. Part A Syst.* **2018**, *144*, 04018038. [CrossRef]
15. Abdulsattar, H.; Mostafizi, A.; Siam, M.R.; Wang, H. Measuring the impacts of connected vehicles on travel time reliability in a work zone environment: An agent-based approach. *J. Intell. Transp. Syst.* **2020**, *24*, 421–436. [CrossRef]
16. Mintsis, E.; Lücken, L.; Karagounis, V.; Porfyri, K.; Rondinone, M.; Correa, A.; Schindler, J.; Mitsakis, E. Joint deployment of infrastructure-assisted traffic management and cooperative driving around work zones. In Proceedings of the 2020 IEEE 23rd International Conference on Intelligent Transportation Systems (ITSC), IEEE, Rhodes, Greece, 20–23 September 2020; pp. 1–8.
17. Jain, S.; Jain, V.; Mishra, S. Probabilistic model for minimizing delay in Vehicular Networks. In Proceedings of the 2023 International Conference on Communication, Circuits, and Systems (IC3S), Bhubaneswar, India, 26–28 May 2023; pp. 1–5. [CrossRef]
18. Popescu, O.; Sha-Mohammad, S.A.; Abdel-Wahab, H.; Popescu, D.; El-Tawab, S. Automatic Incident Detection in Intelligent Transportation Systems Using Aggregation of Traffic Parameters Collected Through V2I Communications. *IEEE Intell. Transp. Syst. Mag.* **2017**, *9*, 64–75. [CrossRef]
19. Jia, D.; Ngoduy, D. Enhanced cooperative car-following traffic model with the combination of V2V and V2I communication. *Transp. Res. Part B Methodol.* **2016**, *90*, 172–191. [CrossRef]
20. Yusuf, S.A.; Khan, A.; Souissi, R. Vehicle-to-everything (V2X) in the autonomous vehicles domain–A technical review of communication, sensor, and AI technologies for road user safety. *Transp. Res. Interdiscip. Perspect.* **2024**, *23*, 100980.
21. Outay, F.; Kammoun, F.; Kaisser, F.; Atiquzzaman, M. Towards safer roads through cooperative hazard awareness and avoidance in connected vehicles. In Proceedings of the 2017 31st International Conference on Advanced Information Networking and Applications Workshops (WAINA), IEEE, Taipei, Taiwan, 27–29 March 2017; pp. 208–215.
22. Huang, Y.; Wang, Y.; Yan, X.; Li, X.; Duan, K.; Xue, Q. Using a V2V-and V2I-based collision warning system to improve vehicle interaction at unsignalized intersections. *J. Saf. Res.* **2022**, *83*, 282–293. [CrossRef]
23. Njobelo, G.; Sando, T.; Sajjadi, S.; Mtoi, E.; Ozguven, E.E.; Sobanjo, J. Safety evaluation of the advanced stop assist system in connected vehicle environment. *Transp. Res. Rec.* **2018**, *2672*, 47–57. [CrossRef]
24. Malinverno, M.; Avino, G.; Casetti, C.; Chiasserini, C.F.; Malandrino, F.; Scarpina, S. Performance analysis of C-V2I-based automotive collision avoidance. In Proceedings of the 2018 IEEE 19th International Symposium on "A World of Wireless, Mobile and Multimedia Networks" (WoWMoM), IEEE, Chania, Greece, 12–15 June 2018; pp. 1–9.
25. Doulabi, S.; Kunnah, H.M.A.; Hassan, H.M. Improving road safety at horizontal curves using V2I speed warning messages. *J. Saf. Res.* **2024**, *88*, 68–77. [CrossRef]
26. Mo, Y.; Vijay, R.; Rufus, R.; Boer, N.d.; Kim, J.; Yu, M. Enhanced perception for autonomous vehicles at obstructed intersections: An implementation of vehicle to infrastructure (v2i) collaboration. *Sensors* **2024**, *24*, 936. [CrossRef] [PubMed]
27. Mukhtar, A.; Xia, L.; Tang, T.B. Vehicle detection techniques for collision avoidance systems: A review. *IEEE Trans. Intell. Transp. Syst.* **2015**, *16*, 2318–2338. [CrossRef]
28. Funke, J.; Brown, M.; Erlien, S.M.; Gerdes, J.C. Collision avoidance and stabilization for autonomous vehicles in emergency scenarios. *IEEE Trans. Control Syst. Technol.* **2016**, *25*, 1204–1216. [CrossRef]
29. Eskandarian, A.; Wu, C.; Sun, C. Research advances and challenges of autonomous and connected ground vehicles. *IEEE Trans. Intell. Transp. Syst.* **2019**, *22*, 683–711. [CrossRef]
30. Choi, K.; Jung, H.G. Cut-in vehicle warning system exploiting multiple rotational images of SVM cameras. *Expert Syst. Appl.* **2019**, *125*, 81–99. [CrossRef]
31. Phan, V.D.; Phan, V.Q.; Dang, T.S.; Trinh, N.H.; Nguyen, P.N.; Luong, N.M.; Nguyen, B.U.; Phan, Q.C.; Bui, H.P.; Nguyen, P.C.A.; et al. Design of Adaptive Fuzzy-PID for Adaptive Cruise Control of Electric Vehicle Using DC Motor: Theory and Experiment. In *Proceedings of the International Conference on Sustainability and Emerging Technologies for Smart Manufacturing*; Springer: Hanoi, Vietnam, 2024; pp. 1–11.
32. Hussan, U.; Majeed, M.A.; Asghar, F.; Waleed, A.; Khan, A.; Javed, M.R. Fuzzy logic-based voltage regulation of hybrid energy storage system in hybrid electric vehicles. *Electr. Eng.* **2022**, *104*, 485–495. [CrossRef]
33. Song, R.; Li, B. Surrounding vehicles' lane change maneuver prediction and detection for intelligent vehicles: A comprehensive review. *IEEE Trans. Intell. Transp. Syst.* **2021**, *23*, 6046–6062. [CrossRef]
34. Prathiba, S.B.; Raja, G.; Kumar, N. Intelligent cooperative collision avoidance at overtaking and lane changing maneuver in 6G-V2X communications. *IEEE Trans. Veh. Technol.* **2021**, *71*, 112–122. [CrossRef]
35. Li, T.; Wu, J.; Chan, C.Y.; Liu, M.; Zhu, C.; Lu, W.; Hu, K. A cooperative lane change model for connected and automated vehicles. *IEEE Access* **2020**, *8*, 54940–54951. [CrossRef]

36. Yi, R.; Yao, Y.; Pu, F.; Zhou, Y.; Wang, X. Cooperative CAV mandatory lane-change control enabled by V2I. *Commun. Transp. Res.* **2024**, *4*, 100126. [CrossRef]
37. Shahriar, M.S.; Kale, A.K.; Chang, K. Enhancing intersection traffic safety utilizing V2I communications: Design and evaluation of machine learning based framework. *IEEE Access* **2023**, *11*, 106024–106036. [CrossRef]
38. Algomaiah, M.; Li, Z. Exploring work zone late merge strategies with and without enabling connected vehicles technologies. *Transp. Res. Interdiscip. Perspect.* **2021**, *9*, 100316. [CrossRef]
39. Agriesti, S.A.M.; Studer, L.; Marchionni, G.; Gandini, P.; Qu, X. Roadworks warning—Closure of a lane, the impact of C-ITS messages. *Infrastructures* **2020**, *5*, 27. [CrossRef]
40. Ren, T.; Xie, Y.; Jiang, L. New England merge: A novel cooperative merge control method for improving highway work zone mobility and safety. *J. Intell. Transp. Syst.* **2021**, *25*, 107–121.
41. Formosa, N.; Quddus, M.; Singh, M.K.; Man, C.K.; Morton, C.; Masera, C.B. An Experiment and Simulation Study on Developing Algorithms for CAVs to Navigate Through Roadworks. *IEEE Trans. Intell. Transp. Syst.* **2023**, *25*, 120–132. [CrossRef]
42. Sommer, C.; German, R.; Dressler, F. Bidirectionally coupled network and road traffic simulation for improved IVC analysis. *IEEE Trans. Mob. Comput.* **2010**, *10*, 3–15.
43. Ormándi, T.; Varga, B. The importance of V2X simulation: An in-depth comparison of intersection control algorithms using a high-fidelity communication simulation. *Veh. Commun.* **2023**, *44*, 100676. [CrossRef]
44. Debalki, Y.A.; Hou, J.; Ullah, H.; Adane, B.Y. Multi-hop data dissemination using a multi-metric contention-based broadcast suppression strategy in VANETs. *Ad Hoc Netw.* **2023**, *140*, 103070.
45. Nour, M.; Zaki, M.H.; Abdel-Aty, M. Towards Connected Smart Work Zones: Advancing Work Zone Management through Improved Connectivity. *arXiv* **2025**, arXiv:2503.14801.
46. Milanés, V.; Shladover, S.E. Modeling cooperative and autonomous adaptive cruise control dynamic responses using experimental data. *Transp. Res. Part C Emerg. Technol.* **2014**, *48*, 285–300.
47. Xie, Y.; Zhang, H.; Gartner, N.H.; Arsava, T. Collaborative merging strategy for freeway ramp operations in a connected and autonomous vehicles environment. *J. Intell. Transp. Syst.* **2017**, *21*, 136–147. [CrossRef]
48. Erdmann, J. SUMO's Lane-Changing Model. In *Proceedings of the Modeling Mobility with Open Data*; Behrisch, M., Weber, M., Eds.; Springer International Publishing: Cham, Switzerland, 2015; pp. 105–123.
49. Dowling, R.; Skabardonis, A.; Alexiadis, V. *Traffic Analysis Toolbox, Volume III: Guidelines for Applying Traffic Microsimulation Modeling Software*; Technical Report; United States Federal Highway Administration Office of Operations: McLean, VA, USA, 2004.
50. Feldman, O. The GEH measure and quality of the highway assignment models. In Proceedings of the Association for European Transport and Contributors, Glasgow, UK, 10–12 October 2012; pp. 1–18.
51. Nezamuddin, N.; Jiang, N.; Zhang, T.; Waller, S.T.; Sun, D. *Traffic Operations and Safety Benefits of Active Traffic Strategies on Txdot Freeways*; Technical Report; National Academies of Sciences: Washington, DC, USA, 2011.
52. Bronner, F.; Sommer, C. Efficient multi-channel simulation of wireless communications. In Proceedings of the 2018 IEEE Vehicular Networking Conference (VNC), IEEE, Taipei, Taiwan, 5–7 December 2018; pp. 1–8.
53. Yang, M.; Wang, X.; Quddus, M. Examining lane change gap acceptance, duration and impact using naturalistic driving data. *Transp. Res. Part C Emerg. Technol.* **2019**, *104*, 317–331. [CrossRef]
54. Hayward, J.C. Near miss determination through use of a scale of danger In *Proceedings of the 51st Annual Meeting of the Highway Research Board*; Highway Research Record, No. 384; Highway Research Board: Washington, DC, USA, 1972; pp. 24–34.
55. Das, S.; Maurya, A.K. Defining Time-to-Collision Thresholds by the Type of Lead Vehicle in Non-Lane-Based Traffic Environments. *IEEE Trans. Intell. Transp. Syst.* **2020**, *21*, 4972–4982. [CrossRef]
56. Sayed, T.; Zein, S. Traffic conflict standards for intersections. *Transp. Plan. Technol.* **1999**, *22*, 309–323. [CrossRef]

Disclaimer/Publisher's Note: The statements, opinions and data contained in all publications are solely those of the individual author(s) and contributor(s) and not of MDPI and/or the editor(s). MDPI and/or the editor(s) disclaim responsibility for any injury to people or property resulting from any ideas, methods, instructions or products referred to in the content.